Equation Chapter 1 Section 1 Analytical Solutions for Radially Functionally Graded Annular Plates

M. H. Babaei[i], M. Salehi[ii] * and R. Naj[iii]

Received 17 June 2008; received in revised 20 July 2010; accepted 14 November 2010

ABSTRACT

A closed-form solution for deflections and stresses in an annular thin plate of radially functionally graded material under transverse uniform pressure loading is presented. The small displacement theory of elasticity is assumed in the present work. Young's modulus of the material is taken in the form of a simple power law to vary in the radial direction with an arbitrary exponent showing heterogeneity of the plate, while Poisson's ratio is held constant throughout the plate. Deflection and stress distributions are graphically presented for various values of the heterogeneity exponent to illustrate its effects on the deflections and stresses. Through the current analysis, this exponent can be adjusted in actual designs to control the deflections and stress levels in a plate.

KEYWORDS

Annular plate, Functionally Graded Material (FGM), Analytical solution

1. INTRODUCTION

Since invented in 1992 [1], functionally graded materials (FGMs) have gained considerable attention, mainly in applications of high temperature and high corrosion environments. FGMs are inhomogeneous but isotropic. Continuous changes in the volume fraction of constituent material leads to smooth changes of material properties including Young's modulus, thermal expansion coefficients, thermal conductivity. Unlike traditional, multilayered composite materials, the smooth change in properties in FGMs helps eliminate the probability of delamination.

As the use of FGMs increases in the aerospace and automotive applications, new methodologies have to be developed to characterize FGMs, and also to design and analyze structural components made of these materials. The methods should be such that they can be incorporated into available methods with least amount of modifications. Although FGMs are highly heterogeneous, it will be useful to idealize them as continua with properties changing smoothly with respect to the spatial coordinates. This will enable us to obtain analytical solutions to some fundamental solid mechanics problems and develop finite-element models for structures of FGMs.

There are some analytical solutions for FGMs. One-dimensional thermal stresses and thermal expansion coefficients of functionally graded sphere and cylinder under uniform heating have been calculated using Ferobenius series with properties changing linearly along the radial coordinate [2,3]. An elasticity solution for FGM beam was proposed and compared with the simpler Euler-Bernoulli solution with the properties changing exponentially in the thickness direction [4]. Assuming power law variations of properties in the radial direction, an exact solution for mechanical stresses was proposed for spherical and cylindrical pressure vessels [5]. Similarly under the same assumption, thermal and mechanical stresses are calculated for one-dimensional case for a cylinder [6]. The same authors solved the problem of functionally graded hollow cylinder due to nonaxisymmetric steady state loads [7]. Using theory of laminated composites, stresses in a cylinder with a finite length were calculated [8]. Recently, the problems of

i M. H. Babaei, PhD, Department of Mechanical Engineering, University of New Brunswick, Fredericton, NB, Canada, E3B 5A3.E-mail: m.babaei@unb.ca

ii * Corresponding Author,M. Salehi, PhD Associate Professor, Department of Mechanical Engineering, Amirkabir University of Technology, 424 Hafez Avenue, Tehran, Iran, 1591634311 E-mail: msalehi@aut.ac.ir

iii R. Naj, M.Sc., Department of Mechanical Engineering, Amirkabir University of Technology, 424 Hafez Avenue, Tehran, Iran, 1591634311.E-mail: reza.naj@gmail.com

axisymmetrically bent functionally graded circular and annular plates were solved using the first-order shear deformation plate theory, and the results were compared with Love-Kirchhoff plate theory [9].

Due to the spatial variation of properties, the number of exact solutions is limited, and numerical methods are widely used to deal with the mechanical behaviour of FGMs. Finite- element method has been used to deal with coupled thermo-mechanical behaviour of FGM plates with variable properties in thickness direction [10], and buckling of FGM plates and shells [11, 12]. One-dimensional steady thermal stresses in functionally graded hollow cylinders and spheres were obtained using perturbation method [13]. Three-dimensional transient thermal stresses of rectangular plate made of FGM due to a partial heat supply, and the piezothermoelastic problem of functionally graded rectangular plate bonded to piezothermoelectric plate, were analyzed using the theory of laminated composites [14, 15].

In this paper, an exact solution for an annular FGM plate under transverse uniform loading was presented. The Love-Kirchhoff assumptions were used to solve the current problem. A radially exponentially graded material model was assumed for the plate. The results for deflections and stresses are presented for different values of the heterogeneity exponent.

2. ANNULAR PLATE GEOMETRY

An annular plate with inner radius *a* and outer radius *b* is subjected to a uniform normal pressure *p*, as shown in Fig.1. A cylindrical coordinate is set up on the plate with (r, θ) coordinates in the plate plane, and z-axis normal to the plate. Young's modulus of the plate varies exponentially in the radial direction such that:

$$\mathrm{E}(r) = E_0 \bar{r}^{\,n} \tag{1}$$

where $\bar{r}$ is the dimensionless radial direction defined later and *n* is called the non-homogeneity index.

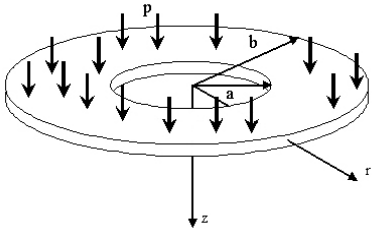

Fig. 1 Plate geometry and positive coordinate system

3. MATHEMATICAL FORMULATION

In order to simplify the derivation and generalize the solution, we introduce the following dimensionless values in the derivations:

$$r = a\bar{r}\,,\ w = t_0\overline{w}\,,\ \ z = t_0\bar{z}\,,\ \ t = t_0\bar{t}\,,\ \ D = D_0\overline{D} \tag{2}$$

where *w* and *D* are the deflection and flexural rigidity of the plate, respectively and t_0 and D_0 are specific thickness and flexural rigidity used to normalize the corresponding parameters. Parameters with overbar indicate dimensionless values.

Using dimensionless values mentioned above, the other quantities will have the following relations:

$$\varepsilon_r = \left(\frac{t_0}{a}\right)^2 \bar{\varepsilon}_r\,,\ \varepsilon_\theta = \left(\frac{t_0}{a}\right)^2 \bar{\varepsilon}_\theta$$

$$M_r = D_0\frac{t_0}{a^2}\overline{M}_r\,,\ M_\theta = D_0\frac{t_0}{a^2}\overline{M}_\theta\,,\ Q_r = D_0\frac{t_0}{a^3}\overline{Q}_r$$

$$p = D_0\frac{t_0}{a^4}\bar{p}\ \ \sigma_r = \frac{D_0}{t_0 a^2}\bar{\sigma}_r\,,\ \ \sigma_\theta = \frac{D_0}{t_0 a^2}\bar{\sigma}_\theta \tag{3}$$

where ε , *M*, *Q* and σ are the strain, bending moment, shear force, and stress, respectively. The quantities with subscripts, *r* and θ indicate the radial and hoop components.

A. Strain-displacement relations

Choosing origin of the coordinates on the middle plane of the plate, (see Fig. 1), mid-plane displacement will be zero and the kinematics relations for non-vanishing strains are given below.

$$\bar{\varepsilon}_r = -\bar{z}\frac{d^2\overline{w}}{d\bar{r}^2} \tag{4}$$

$$\bar{\varepsilon}_\theta = -\frac{\bar{z}}{\bar{r}}\frac{d\overline{w}}{d\bar{r}} \tag{5}$$

B. Constitutive Equations

The dimensionless stress-strain relations are as follows:

$$\bar{\sigma}_r = \frac{\bar{E}}{1-\nu^2}\left(\bar{\varepsilon}_r + \nu\bar{\varepsilon}_\theta\right) \tag{6}$$

$$\bar{\sigma}_\theta = \frac{\bar{E}}{1-\nu^2}\left(\bar{\varepsilon}_\theta + \nu\bar{\varepsilon}_r\right) \tag{7}$$

where ν is Poisson's ratio which is taken to be constant in the current work.

Substituting Eq. (4) and Eq. (5) into Eq. (6) and Eq. (7), the stresses become:

$$\bar{\sigma}_r = -\frac{\bar{E}\bar{z}}{1-\nu^2}\left(\frac{d^2\overline{w}}{d\bar{r}^2} + \frac{\nu}{\bar{r}}\frac{d\overline{w}}{d\bar{r}}\right) \tag{8}$$

$$\bar{\sigma}_\theta = -\frac{\bar{E}\bar{z}}{1-\nu^2}\left(\nu\frac{d^2\overline{w}}{d\bar{r}^2} + \frac{1}{\bar{r}}\frac{d\overline{w}}{d\bar{r}}\right) \tag{9}$$

Multiplying these equations by *z* and then integrating over the thickness, we have the following results for the stress couples:

$$\overline{M}_r = -\overline{D}\left(\frac{d^2\overline{w}}{d\bar{r}^2} + \frac{\nu}{\bar{r}}\frac{d\overline{w}}{d\bar{r}}\right) \tag{10}$$

$$\overline{M}_\theta = -\overline{D}\left(\nu\frac{d^2\overline{w}}{d\bar{r}^2} + \frac{1}{\bar{r}}\frac{d\overline{w}}{d\bar{r}}\right) \tag{11}$$

C. Equilibrium Equations

A plate element showing the forces and moments is depicted in Fig. 2.

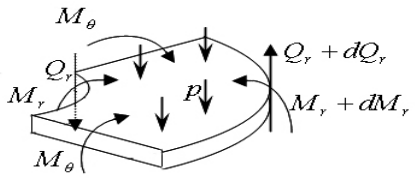

Fig. 2 Plate element

From the equilibrium in the transverse direction, we have:

$$\bar{p} + \frac{\bar{Q}_r}{\bar{r}} + \frac{d\bar{Q}_r}{d\bar{r}} = 0 \tag{12}$$

For moment balance, we have:

$$\frac{\bar{M}_r - \bar{M}_\theta}{\bar{r}} + \frac{d\bar{M}_r}{d\bar{r}} = \bar{Q}_r \tag{13}$$

Substituting Eq. (10) and Eq. (11) for $\bar{M}_r$ and $\bar{M}_\theta$ into Eq. (13) gives:

$$\bar{Q}_r = -\bar{D}\frac{d^3\bar{w}}{d\bar{r}^3} - \left(\frac{1}{\bar{r}}\bar{D} + \frac{d\bar{D}}{d\bar{r}}\right)\frac{d^2\bar{w}}{d\bar{r}^2} + \left(\frac{1}{\bar{r}^2}\bar{D} - \frac{\nu}{\bar{r}}\frac{d\bar{D}}{d\bar{r}}\right)\frac{d\bar{w}}{d\bar{r}} \tag{14}$$

Substituting Eq. (14) for $\bar{Q}_r$ into Eq. (12) leads to the governing differential equation for the plate:

$$\bar{D}\frac{d^4\bar{w}}{d\bar{r}^4} + 2\left(\frac{1}{\bar{r}}\bar{D} + \frac{d\bar{D}}{d\bar{r}}\right)\frac{d^3\bar{w}}{d\bar{r}^3} + \left(-\frac{1}{\bar{r}^2}\bar{D} + \frac{2+\nu}{\bar{r}}\frac{d\bar{D}}{d\bar{r}} + \frac{d^2\bar{D}}{d\bar{r}^2}\right)\frac{d^2\bar{w}}{d\bar{r}^2} + \left(\frac{1}{\bar{r}^3}\bar{D} - \frac{1}{\bar{r}^2}\frac{d\bar{D}}{d\bar{r}} + \frac{\nu}{\bar{r}}\frac{d^2\bar{D}}{d\bar{r}^2}\right)\frac{d\bar{w}}{d\bar{r}} = \bar{p} \tag{15}$$

Following Eq. (1), the flexural rigidity can be assumed to obey power law as well:

$$D(r) = D_0 r^n \tag{16}$$

Substituting Eq. (16) into Eq. (15) yields:

$$\bar{r}^4\frac{d^4\bar{w}}{d\bar{r}^4} + 2(1+n)\bar{r}^3\frac{d^3\bar{w}}{d\bar{r}^3} + \left(n^2 + n(1+\nu) - 1\right)\bar{r}^2\frac{d^2\bar{w}}{d\bar{r}^2} + \left(\nu n^2 - n(1+\nu) + 1\right)\bar{r}\frac{d\bar{w}}{d\bar{r}} = \bar{p}\bar{r}^{4-n} \tag{17}$$

"Equation (17) is a fourth-order Euler-Cauchy non-homogeneous differential equation with variable coefficients.

Now, we use a change of variable in the form of $\bar{r} = e^t$, where t is a new variable. The homogeneous part of Eq. (17) will be then rewritten as:

$$w'''' + 2(n-2)w''' + \left(n^2 + (\nu-5)n + 4\right)w'' + (\nu-1)n(n-2)w' = 0 \tag{18}$$

where $(\ )' = \frac{d}{dt}(\ )$

The corresponding characteristic equation for Eq. (18) becomes

$$m^4 + 2(n-2)m^3 + \left(n^2 + (\nu-5)n + 4\right)m^2 + (\nu-1)n(n-2)m = 0 \tag{19}$$

The four nontrivial roots of this algebraic equation are:

$$m_1 = 0 \tag{20}$$
$$m_2 = -n + 2$$
$$m_3 = -\frac{n}{2} + 1 + \frac{\sqrt{n^2 + 4 - 4n\nu}}{2}$$
$$m_4 = -\frac{n}{2} + 1 - \frac{\sqrt{n^2 + 4 - 4n\nu}}{2}$$

In general, the solution of the fourth-order algebraic equation results in four different roots, i.e. m_1, m_2, m_3 and m_4 hence the general solution of Eq. (17) becomes

$$\bar{w}_g(\bar{r}) = A_1\bar{r}^{m_1} + A_2\bar{r}^{m_2} + A_3\bar{r}^{m_3} + A_4\bar{r}^{m_4} \tag{21}$$

We assume the particular solution of the Eq. (17) to be of the form:

$$\bar{w}_p(\bar{r}) = B_1\bar{r}^{4-n} \tag{22}$$

Using the particular solution in Eq. (17), the value for B_1 is obtained as follows:

$$B_1 = -\frac{\bar{p}}{2(n-4)\left(n(\nu-3)+8\right)} \tag{23}$$

Consequently, the solution for the non-homogeneous differential equation is the sum of the general and the particular solutions:

$$\bar{w} = \bar{w}_g + \bar{w}_p \tag{24}$$

and the final result is:

$$\bar{w} = A_1\bar{r}^{m_1} + A_2\bar{r}^{m_2} + A_3\bar{r}^{m_3} + A_4\bar{r}^{m_4} - \frac{\bar{p}}{2(n-4)\left(n(\nu-3)+8\right)}\bar{r}^{4-n} \tag{25}$$

4. BOUNDARY CONDITIONS

Now we can apply an arbitrary boundary condition. The four coefficients in Eq. (25) can be determined using four independent boundary conditions. Boundary conditions can be of various forms: if they are given in terms of displacement, Eq. (25) should be used directly; but if they are given in terms of stress (or moment) or shear forces, we should introduce Eq. (25) into the corresponding physical equation mentioned before, and then, apply boundary conditions to find the four coefficients, A_i's.

Two illustrative examples are given below:

Problem (1): Inner surface is clamped while the outer surface is free hence we have:

$$\text{at r = a} \quad \begin{cases} w = 0 \\ \dfrac{dw}{dr} = 0 \end{cases} \quad \text{and at r= b} \quad \begin{cases} M_r = 0 \\ Q_r = 0 \end{cases}$$

Problem (2): Inner surface at $r = a$, is simply supported and the outer surface at $r = b$ is clamped. Thus, we have:

$$\text{at r = a} \quad \begin{cases} w = 0 \\ M_r = 0 \end{cases} \quad \text{and at r = b} \quad \begin{cases} w = 0 \\ \dfrac{dw}{dr} = 0 \end{cases}$$

With these four conditions, the boundary value problem is completely solved and the results for deflections, radial stresses and circumferential stresses are given in Figures 3 to 5.

5. NUMERICAL RESULTS

In order to generate numerical results for various n values the analytical results are plugged into the Matlab computer software. In each example problem, the numerical results for transverse displacements, normalized radial and hoop stresses are plotted along the radial line of the plate. The values of the non-homogeneity index are in the range of -2 to +2 in steps of 1. However, it is worth pointing out that these values for n do not necessarily represent a certain material. Various n values are applied to demonstrate the effect of inhomogeneity on the transverse displacement and stress distribution. A positive value of n means increasing stiffness in the radial direction. In addition, the results for isotropic plate ($n=0$) are shown simultaneously for the purpose of comparison.

The transverse displacements are illustrated in Fig. 3 for an annular plate with a clamped inner edge and a free outer edge. As the value of n changes from -2 to +2, the deflections decrease. This result reveals that by stiffening the plate in the radial direction going from the inner to the outer edge, the deflections of the plate will decrease.

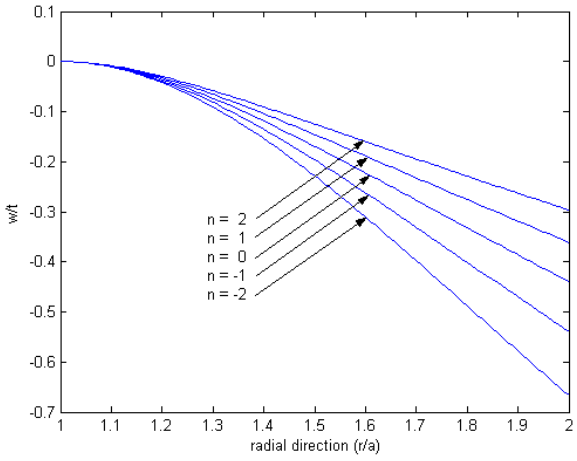

Fig. 3 Dimensionless deflections along the plate radius, the plate is clamped at the inner edge while the other edge is free

The normalized radial and circumferential stresses are illustrated in Fig. 4a and Fig. 4b for the same plate. The radial stress reaches its maximum at the clamped edge and drops to zero towards the outer edge. For a less stiffer material, the stresses at the inner edge are higher than the stresses for a stiffer material. For the hoop stress, an increase in positive values of n results in smoother variations in stress along the radius of the plate.

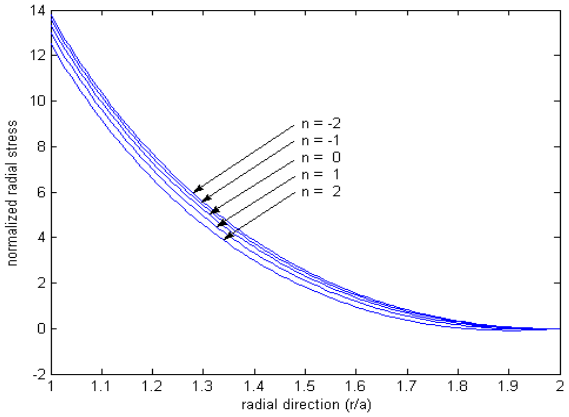

(a)

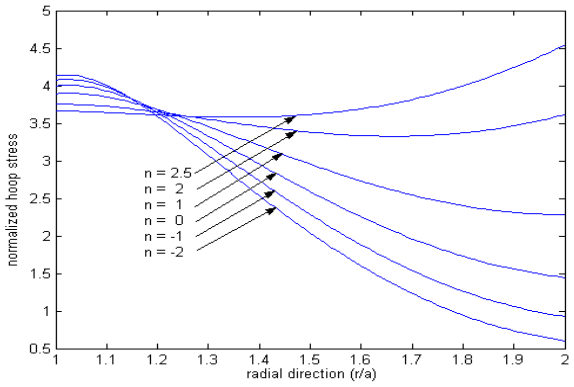

(b)

Fig. 4 Normalized stress distributions along the plate radius, the plate is clamped at the inner edge while the other edge is free, a) radial stresses b) hoop stresses

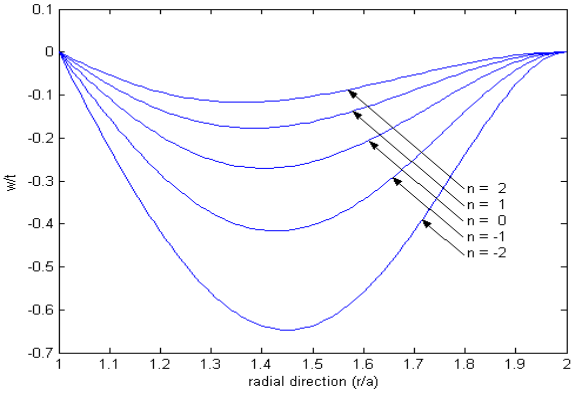

(a)

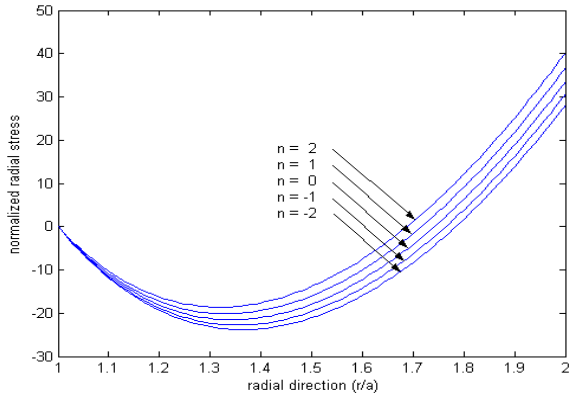

(b)

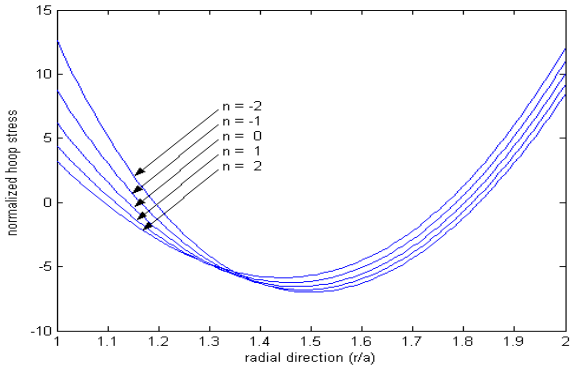

(c)

Fig. 5 Deflection and stress distributions along the plate radius, the plate is simply supported at the inner edge while clamped at the other edge, a) Non-dimensional deflections b) Normalized radial stresses c) Normalized hoop stresses

Figure 5a illustrates the deflections for an annular plate, simply supported at the inner edge and clamped at the outer edge. An Increase in *n* results in a decrease in the deflection. Figure 5b and Figure 5c illustrate the normalized radial and hoop stresses for the plate under the same boundary conditions, respectively. The radial stresses are zero at the inner edge, while at the outer edge, a higher radial stress occurs for a stiffer plate while a lower radial stress for a less stiffer plate. The maximum positive radial stress occurs at the outer edge and the maximum negative radial stress occurs at nearly the middle of the plate between the inner and outer edges. In the case of hoop stresses, the same behaviour is observed with the positive stress of maximum magnitude occurring at the inner edge for a negative *n* value, and the negative stress of maximum magnitude occurs close to the middle of the plate between the inner and outer edges.

6. CONCLUSIONS

An analytical solution for an annular plate of radially functionally graded material was presented in this paper. In the framework of small displacement elasticity theory, the fourth-order Euler Cauchy equation was developed for the plate. The analytical solution of this equation resulted in the expression of the transverse displacement, or normal deflection. Two different boundary conditions were considered to obtain the solutions. The numerical results illustrated for deflections and stresses imply that the non-homogeneity index, *n*, can be used to control the deflections and stresses of the plate in the actual design.

7. REFERENCES

[1] M.Yamanouchi, M. Koizumi, T. Hirai, and I. Shiota (eds.), Proc. First Int.Sympos, Functionally Gradient Materials, Japan, 1990.

[2] Melanie P. Lutz, Robert W. Zimmerman, "Thermal stresses and effective thermal expansion coefficient of a functionally graded sphere", J. Thermal Stresses, Vol. 19, 1996, pp. 39-54.

[3] Robert W. Zimmerman, Melanie P. Lutz, "Thermal stresses and thermal expansion in a uniformly heated functionally graded cylinder", J. Thermal Stresses, Vol. 22, 1999, pp. 177-188.

[4] B. V. Sankar, "An elasticity solution for functionally graded beams", J. Composites Science and Technology, Vol. 61, 2001, pp. 686-696.

[5] Naki Tutuncu, Murat Ozturk, "Exact solutions for stresses in functionally graded pressure vessels", J. Composites Part B: Engineering, Vol. 32, 2001, pp. 683-686.

[6] M. Jabbari, S. Sohrabpour, M. R. Eslami, "Mechanical and thermal stresses in a functionally graded hollow cylinder due to radially symmetric loads", Int. J. Pressure Vessels and Piping, Vol. 79, 2002, pp. 493-497.

[7] M. Jabbari, S. Sohrabpour, M. R. Eslami, "General solution for mechanical and thermal stresses due to nonaxisymmetric steady-state loads", ASME J. Applied Mechanics, Vol. 70, 2003, pp. 111-118.

[8] Z.S. Shao, "Mechanical and thermal stresses of functionally graded circular hollow cylinder with finite length", Int. J. Pressure Vessels and Piping, Vol. 82, 2005, pp. 155-163.

[9] J. N. Reddy, C. M. Wang, S., "Kitipornchai. Axisymmetric bending of functionally graded circular and annular plates", Eur. J. Mech. A/Solids, Vol. 18, 1999, pp. 185-199.

[10] J. N. Reddy, C. D. Chin, "Thermomechanical analysis of functionally graded cylinders and plates", J. Thermal Stresses, Vol. 21, 1998, pp. 593-626.

[11] R. Shahsiah, M.R. Eslami, "Thermal instability of functionally graded cylindrical shell based on the improved Donnell equations", AIAA J., Vol. 41(9), 2003, pp. 1819-1827.

[12] R. Javaheri, M.R. Eslami, "Thermal buckling of functionally graded plates", AIAA J., Vol. 40(1), 2002, pp. 162-169.

[13] Y. Obata, N. Noda, "Steady thermal stresses in a hollow circular cylinder and a hollow sphere of a functionally graded material", J. Thermal Stresses, Vol. 17, 1994, pp. 471-487.

[14] Y. Ootao, Y. Tanigawa, "Three-dimensional transient thermal stresses of functionally graded rectangular plate due to partial heating", J. Thermal Stresses, Vol. 22, 1999, pp. 35-55.

[15] Y. Ootao, Y. Tanigawa, "Three-dimensional transient piezothermoelasticity in functionally graded rectangular plate bonded to a piezoelectric plate", Int. J. Solids and Structures, Vol. 37, 2000, pp. 4377-4401.